NANO LETTERS

2007
Vol. 7, No. 4
905−909

Probing the Local Coordination Environment for Transition Metal Dopants in Zinc Oxide Nanowires

Benjamin D. Yuhas,[†] Sirine Fakra,[‡] Matthew A. Marcus,[‡] and Peidong Yang*[,†,§]

Department of Chemistry, University of California, Berkeley, California 947202, Advanced Light Source, Lawrence Berkeley National Laboratory, Berkeley, California 947203, and Materials Sciences Division, Lawrence Berkeley National Laboratory, Berkeley, California 94720

Received November 17, 2006; Revised Manuscript Received February 8, 2007

ABSTRACT

It is hypothesized that a highly ordered, relatively defect-free dilute magnetic semiconductor system should act as a weak ferromagnet. Transition-metal-doped ZnO nanowires, being single crystalline, single domain, and single phase, are used here as a model system for probing the local dopant coordination environments using X-ray absorption spectroscopy and diffraction. Our X-ray spectroscopic data clearly show that the dopant resides in a uniform environment, and that the doping does not induce a large degree of disorder in the nanowires. This homogeneous nature of the doping inside the oxide matrix correlates well with observed weakly ferromagnetic behavior of the nanowires.

Dilute magnetic semiconductors are of great current research interest owing to their novel magnetic properties. These materials are envisioned to have potential use in so-called "spintronic" devices, in which one seeks to control both the charge and spin degrees of freedom of the electron; a few such prototypical devices are already in existence.[1,2] Despite improvements in device fabrication, the fundamental questions regarding the origins of the magnetic behavior in dilute magnetic semiconducting (DMS) systems remain unsatisfactorily answered. It is known that much of the controversy has stemmed from the fact that clustering or phase separation of the magnetic dopant ions can result in magnetic data that is misleading or unreliable.[3−5] Even in systems that appear to be quite pure, reported magnetic behavior can vary widely, ranging from room-temperature ferromagnetism[6] to no magnetic ordering at all.[7,8] This variance in magnetism is attributed to the multitude of synthetic methods used for the production of DMS materials, which can result in differences in dopant environment, structural disorder, or carrier concentration. Therefore, to extract the most accurate information from any magnetic data on a DMS material, it is vital to perform a rigorous structural characterization.

A combination of X-ray spectro-microscopy and X-ray diffraction (XRD) techniques can provide excellent insight into the structure of a DMS system, down to the local environment of the magnetic cation. Although these types of experiments have been conducted previously on bulk and thin film systems of DMS materials,[9−12] very few studies on one-dimensional nanostructures of transition-metal (TM)-doped semiconductors have been reported. In this Letter, we report results of a detailed structural analysis on TM-doped (Co and Mn) ZnO nanowires grown by a novel solution-based synthesis, and we correlate these findings with the magnetic properties of the nanowires. *These transition-metal-doped ZnO nanowires, being single crystalline, single domain, and single phase, serve as an excellent model system for probing the local dopant coordination environments and their correlation with magnetic properties.* XRD, micro-extended X-ray absorption fine structure spectroscopy (μ-EXAFS), as well as high-resolution imaging combined with near-edge X-ray absorption fine structure (NEXAFS) spectroscopy using scanning transmission X-ray microscopy (STXM), were conducted at the Advanced Light Source (ALS) at Lawrence Berkeley National Laboratory.

The TM-doped nanowires used in this study were synthesized as previously reported.[13] Zinc acetate and the desired TM(II) acetate were dissolved in trioctylamine at 310 °C and reacted for 3 h. The nanowires had uniform diameters of 35 ± 5 nm, and lengths ranging from 2 to 6 μm, depending on the type and amount of TM dopant. Average dopant concentrations were determined by energy-dispersive X-ray spectroscopy (EDX) in a Philips CM200 transmission electron microscope. The standard deviations in dopant concentration were consistently ∼9−10% of the mean value. We also observed no lateral or longitudinal dopant concen-

[†] Department of Chemistry, University of California.
[‡] Advanced Light Source.
[§] Material Sciences Division, Lawrence Berkeley National Laboratory.

10.1021/nl0626939 CCC: $37.00
Published on Web 03/03/2007

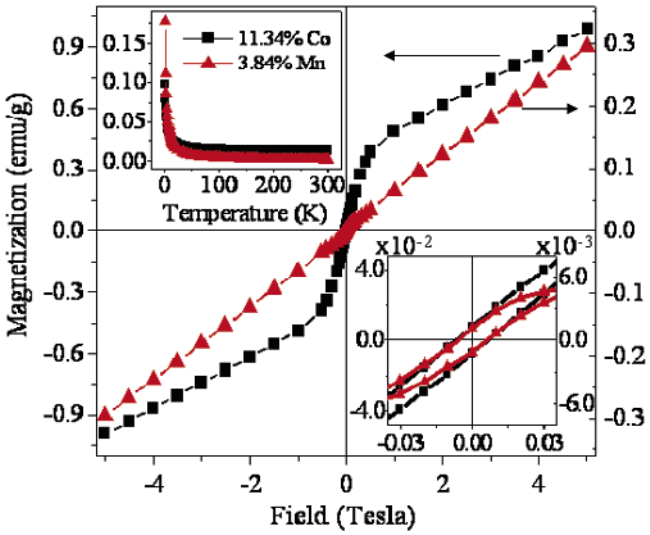

Figure 1. (A) M−H plot of 11.34% Co-doped (■, left axis) and 3.84% Mn-doped (▲, right axis) nanowires at 300 K. Inset: *M*−*T* plot at 500 G.

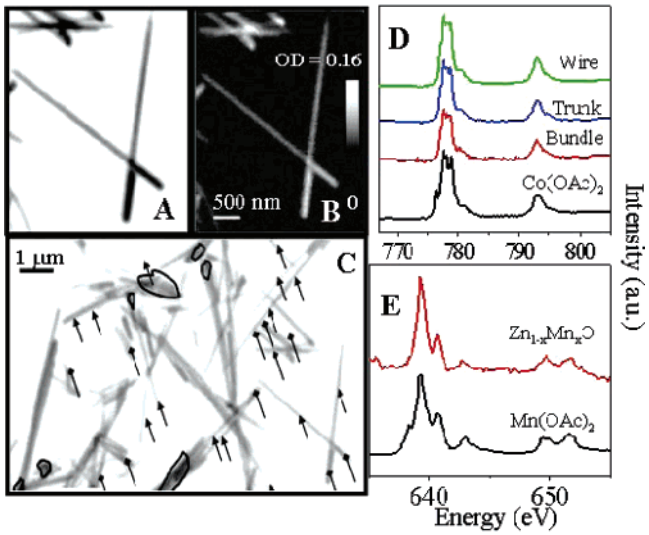

Figure 2. (A) STXM image of $Zn_{1-x}Co_xO$ nanowire bundles; $x = 0.0671$. Transmission image obtained at Co L_3 edge (778 eV). (B) Co elemental map, obtained from difference of optical density (OD) images recorded at 778 and 765 eV on area *A*. (C) STXM image of a larger dispersion of the nanowire sample, taken at the Co L_3 edge. Circled areas denote "bundle" Co NEXAFS spectra, diamond arrows denote "trunk" spectra, and pointed arrows denote "wire" spectra in (D). (E) NEXAFS spectra for a $Zn_{1-x}Mn_xO$ nanowire sample; $x = 0.0312$.

tration gradient by EDX in any of the nanowire samples.[13] The nanowire magnetic properties were measured in powder form using a SQUID magnetometer (Quantum Design MPMS XL); the results are displayed in Figure 1. Both the Co and Mn-doped wires can be described as weak ferromagnets with an additional paramagnetic component. Each sample, regardless of dopant concentration, exhibits a small hysteresis near the origin, but at higher applied fields, paramagnetic behavior is observed, as evidenced by the linear shape of the M−H curve. Temperature-dependent magnetization measurements support the idea of the nanowires possessing paramagnetic and ferromagnetic components, with one dominating over the other at different temperatures.

To characterize the local environment and distribution of the dopant in the nanowires, we performed STXM-based NEXAFS spectroscopy at ALS Beamline 11.0.2.[14] High-resolution imaging (∼40 nm spatial resolution) was carried out at the TM $L_{2,3}$ edges with a theoretical spectral resolution of 0.1 eV. Differences of optical density images, recorded at energies below and at the relevant absorption edge, were used to derive elemental maps.[15] Series of transmission images were acquired across the TM $L_{2,3}$ edges and NEXAFS spectra were extracted from various regions of interest on the doped nanowires using the aXis-2000 software.[16] Figure 2A,B shows a transmission image along with the corresponding elemental map obtained on a $Zn_{1-x}Co_xO$ nanowire sample. In all cases, we observed a uniform X-ray absorption signal, both across several nanowire bundles as well as within a single bundle, implying that the dopant is very evenly distributed throughout the nanowire sample, which is consistent with our previous EDX observations.[13] Differences in intensity can be attributed to the varying thickness of the nanowire sample; this is a consequence of the growth mechanism, which features several nanowires growing in a pan-pipe geometry from a common, thicker hexagonal base.[13]

Figure 2D shows the cobalt NEXAFS spectra obtained from various regions in the nanowire samples (Figure 2C), along with that of the cobalt precursor, cobalt(II) acetate. The peak positions and the line shape of the spectra depend on the local electronic structure of the Co ion, providing information on the valence state and the site symmetry. The Co $L_{2,3}$ lines are separated by the large 2p core−hole spin−orbit interaction, and the core−hole lifetime broadening is small, resulting in sharp multiplet structures. No energy shift is observed in the absorption edges between the precursor and the nanowires, which indicates that the Co cations in the nanowires are divalent. Also, the acetate has a sharp preedge feature at the L_3 edge, which is missing in the nanowires. This preedge feature has been attributed to the presence of an inversion center;[17] we thus see that the TM coordination in the nanowire is not octahedral, unlike in the precursor. A tetrahedral coordination is readily confirmed by electronic absorption or photoluminescence spectroscopy,[13,18−20] as well as the EXAFS measurements discussed below. Finally, we observe identical NEXAFS transmission spectra whether we collect from the trunk region of the nanowire bundles or the individual nanowires themselves, regardless of the concentration or identity of the dopant. This suggests that there is no significant variance in dopant environment throughout the nanowires, which is reasonable considering observations during nanowire growth.[13] For example, early in the Co-doped nanowire synthesis, the solution turns royal blue as the precursors dissolve, which is characteristic of the Co^{2+} ion in tetrahedral coordination.[21] It seems likely then, as the zinc acetate precursor decomposes and forms ZnO, that the TM ions are captured into the growing crystal lattice and retain their tetrahedral geometry in the wurtzite crystal structure. However, with this method alone, we cannot exclude the possibility of very small amounts of dopants residing in coordination environments other than tetrahedral, particularly on the surface of the

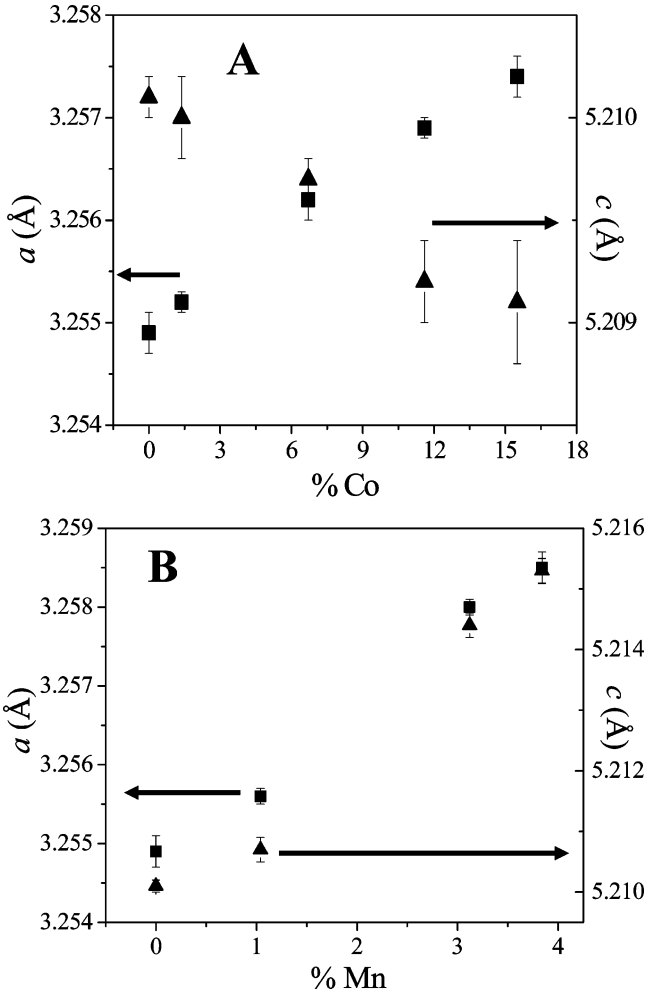

Figure 3. Lattice constants for (A) $Zn_{1-x}Co_xO$ and (B) $Zn_{1-x}Mn_xO$ nanowires. Square markers correspond to the *a* parameter, and triangle markers correspond to the *c* parameter.

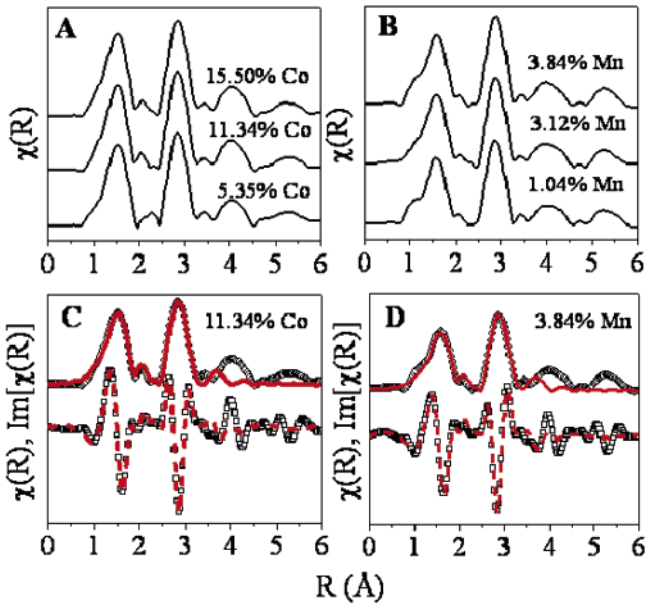

Figure 4. (A), (B) Magnitude of the Fourier-transformed TM K-edge EXAFS spectra. (C), (D) Comparisons between experimental data (○, magnitude; □, imaginary part) and the FEFF fit in the range 1.0−3.4 Å. All spectra are vertically offset for clarity.

nanowires. The role of surface dopants on the magnetic properties of DMS materials is not clearly defined and remains an area of active debate. Although we know from previous studies that the TM dopants do not accumulate at the nanowire surface,[13] the transmission geometry of the NEXAFS experiment makes it impossible to distinguish between a TM dopant on the surface and one in the interior of the nanowire.

NEXAFS measurements can provide information such as dopant oxidation state and crystal field in the nanowires with excellent resolution, but they cannot detect subtle differences in the environment around the dopant, such as lattice distortion. To investigate this possibility, we conducted XRD measurements at ALS Beamline 11.3.1. The nanowires were isolated as a powder sample and mixed with silicon powder (NIST 660b) to provide internal calibration. Diffraction patterns were recorded in transmission mode using an incident photon energy of 17 keV ($\lambda = 0.73$ Å). The Bragg peaks were fitted to Pearson-VII functions, and the lattice constants were calculated from a least-squares analysis of the Bragg peak positions. Figure 3 shows the variation of the nanowire lattice constant as a function of TM concentration. In all cases, the only observed phase was that of wurtzite ZnO. For the case of $Zn_{1-x}Mn_xO$, there is an expansion in the lattice constant, as would be expected with the substitution of the larger Mn^{2+} cation (~0.66 Å) for the Zn^{2+} cation (~0.60 Å). The case of $Zn_{1-x}Co_xO$, however, is more unusual in that although the *c* parameter shrinks, the *a* lattice parameter expands. As Co^{2+} is a smaller cation (~0.56 Å) than Zn^{2+}, one would expect lattice contraction to occur. This anomalous lattice expansion in $Zn_{1-x}Co_xO$ has been previously reported in studies of bulk $Zn_{1-x}Co_xO$ powders,[22] where the expansion of the *a* lattice parameter was attributed to possible interstitial coordination of Co^{2+} dopant cations. In our case, it is also possible that the doping induces a localized distortion of the lattice around the dopant. To explore these possibilities, we performed K-edge EXAFS spectroscopy at ALS Beamline 10.3.2.[23]

A series of EXAFS absorption spectra was collected at the TM K-edges using a beam spot size of 5 μm × 5 μm. The EXAFS spectra were background substracted and normalized using ATHENA.[24] The k^2-weighted EXAFS spectra were Fourier transformed with a Kaiser−Bessel window to real (R) space; the results are displayed in Figure 4. In all cases, the Fourier transforms are similar in appearance, with no extraneous peaks or changes in peak position as the dopant concentration increases. Additionally, we are able to observe at least four coordination shells contributing to the EXAFS. The spectra suggest that the doped nanowires are a highly ordered system, without a high level of dopant-induced defects, even at very high TM concentrations. The EXAFS spectra were modeled theoretically using FEFF 8.0 within the modeling program ARTEMIS.[24] The model used was the standard wurtzite structure of ZnO, with the central atom changed to the appropriate transition metal. The lattice parameters used were those extracted from the XRD experiments. Alternate values of *a* and *c*, such as those from literature or a differently doped

Table 1. EXAFS Fitting Parameters[a]

sample	11.34% Co	11.34% Co	3.84% Mn	3.84% Mn
spectrum	Co K-edge	Zn K-edge	Mn K-edge	Zn K-edge
R-factor	0.0062	0.0074	0.0092	0.0076
R_{M-O1} (Å) $N=1$	1.942 ± 0.005	1.930 ± 0.004	1.999 ± 0.008	1.932 ± 0.005
R_{M-O2} (Å) $N=3$	1.977 ± 0.005	1.965 ± 0.005	2.035 ± 0.008	1.967 ± 0.005
R_{M-M1} (Å) $N=6$	3.203 ± 0.004	3.201 ± 0.004	3.219 ± 0.006	3.205 ± 0.004
R_{M-M2} (Å) $N=6$	3.246 ± 0.004	3.245 ± 0.004	3.264 ± 0.006	3.247 ± 0.004
$\sigma^2_O(10^{-3}$ Å$^2)$	2.87 ± 1.07	4.71 ± 1.30	3.41 ± 1.22	5.01 ± 1.49
$\sigma^2_M(10^{-3}$ Å$^2)$	8.03 ± 0.83	8.42 ± 0.95	8.65 ± 1.04	9.07 ± 0.98

[a] R is the distance from the absorbing atom to an oxygen or cation neighbor, σ^2 is the mean-square displacement of the scattering atoms. The degeneracies N were held constant.

nanowire sample, consistently resulted in lower-quality fits. Fitting was restricted to the first two coordination shells, in the range from 1.0 to 3.4 Å, and a k-range from 2.5 to 11.0 Å^{-1}.

Table 1 lists the calculated nearest-neighbor distances from fits of both the TM K-edge spectra and the Zn K-edge spectra (not shown). The concentration of dopant in the nanowires did not greatly affect the calculated distances (<0.01 Å across concentrations), but there are significant changes in distance between the Co-doped and the Mn-doped nanowires. In the Mn-doped wires, there is a significant expansion in the Mn−O first shell distance compared to the Zn−O distance. This is reasonable given the relative sizes of the cations and is consistent with the expansion of the lattice parameters we observed from XRD. The Co-doped nanowires also show an increase in the Co−O distance relative to the Zn−O distance, although the magnitude of this increase is not as large as in the Mn-doped wires. Additionally, the second-shell distances in the Co-doped wires are similar when calculated from either the Co K-edge or the Zn K-edge, whereas this is not the case in the Mn-doped wires. This suggests that the TM dopant induces a local lattice distortion that is compensated by the surrounding atoms, and that this distortion is greater for the Mn-doped nanowires. It is unclear if the amount of distortion or the average bond distance varies in different sections of the nanowire (i.e., the "trunk" or "wire" regions as defined above), as our EXAFS data, which represent an average over a macroscopic volume of nanowires, cannot satisfactorily address this issue. The difference in the distortion between different TM dopants could also explain why wires with Co concentration exceeding ten atomic percent can be readily synthesized, but the maximum attainable Mn concentration in our nanowires is under four atomic percent. Nevertheless, the EXAFS analysis suggests that any lattice distortions in the TM-doped nanowires are confined locally around the dopants, with no widespread, systematic defects arising in the ZnO lattice due to TM doping.

These observations concerning the local structure and environment of the dopant have important consequences regarding the observed magnetic properties of the nanowires. It has been shown for DMS systems that the amount of structural disorder, both locally around the dopant and throughout the entire semiconductor, can have a profound effect on magnetic properties.[25−27] Theoretical studies predict that a highly ordered, relatively defect-free DMS system will act as a weak ferromagnet.[28] According to the bound magnetic polaron theory,[29] the spins of the magnetic transition metal cations are aligned by the spins of carriers localized on lattice defects. If the defect density is low relative to the TM dopant concentration, as our experiments indicate, the degree of magnetic ordering will also be low. This is precisely what we have observed in our magnetic measurements. The spins that do not participate in ferromagnetic ordering could act as simple paramagnets if they are sufficiently isolated, or they could be paired antiferromagnetically if two of them are in close proximity.

First-principles calculations[30] show that paired magnetic cations in $Zn_{1-x}Co_xO$ tend to align antiferromagnetically in the absence of any other influence. Increasing the level of dopant concentration in our nanowires does not produce a concurrent increase in defect density, as shown by the EXAFS. As higher levels of magnetic cations are doped into the nanowires without a significant increase in the defect density, there will likely be a greater number of antiferromagnetic pairs of cations, which would cause a drop in the overall magnetic moment per dopant in the nanowires. This has actually been repeatedly observed in our concentration dependent magnetic measurements, for both Co- and Mn-doped wires.

Our detailed structural analysis allows for a direct correlation between the local atomic structure of a DMS material and its magnetic properties. We find that magnetic dopants are homogeneously distributed within our single crystalline, single phase ZnO nanowires and adopt a highly uniform local coordination environment. These transition-metal-doped nanowires exhibit weak ferromagnetism, which validates theoretical predictions of magnetism in TM-doped ZnO. A thorough understanding of the correlation between the atomic structures of the DMS materials and their magnetic properties should provide important insights on the high-temperature ferromagnetism in these transition-metal-doped oxide systems.

Acknowledgment. This work was supported by the Department of Energy and the Western Institute of Nanoelectronics (WIN). We thank Prof. Jeff Long for the use of the SQUID magnetometer. S.F. thanks Tolek Tyliszczak, Mary K. Gilles, and D. K. Shuh for providing beamtime at beamline 11.0.2. Work at the Lawrence Berkeley National Laboratory was supported by the Office of Science, Basic Energy Sciences, Division of Materials Science, of the U.S. Department of Energy under contract number DE-AC02-05CH11231.

References

(1) Kioseoglou, G.; et al. *Nat. Mater.* **2004**, *3*, 799.
(2) Chakrabarti, S.; et al. *Nano Lett.* **2005**, *5*, 209.
(3) Kundaliya, D. C.; et al. *Nat. Mater.* **2004**, *3*, 709.
(4) Park, J. H.; et al. *Appl. Phys. Lett.* **2004**, *84*, 1338.
(5) Kim, J. H.; et al. *J. Eur. Ceram. Soc.* **2004**, *24*, 1847.
(6) Ramachandran, S.; Tiwari, A.; Narayan, J. *Appl. Phys. Lett.* **2004**, *84*, 5255.
(7) Jedrecy, N.; et al. *Phys. Rev. B* **2004**, *69*, 41308.

(8) Lawes, G.; et al. *Phys. Rev. B* **2005**, *71*, 45201.
(9) Keavney, D. J.; et al. *Phys. Rev. Lett.* **2005**, *95*, 257201.
(10) Schuler, T. M.; et al. *Phys. Rev. B* **2005**, *72*, 045211.
(11) Wi, S. C.; et al. *Appl. Phys. Lett.* **2004**, *84*, 4233.
(12) Lussier, A.; et al. *J. Appl. Phys.* **2004**, *95*, 7190.
(13) Yuhas, B. D.; et al. *Angew. Chem. Int. Ed.* **2006**, *45*, 420.
(14) Kilcoyne, A. L. D.; et al. *J. Synchrotron Rad.* **2003**, *10*, 125.
(15) Optical density (OD) is defined as OD $= -\ln(I/I_0)$, where I and I_0 are the transmitted and incident X-ray intensities, respectively.
(16) A. P. Hitchcock (2000), aXis-2000 is an IDL-based analytical package. http://unicorn.mcmaster.ca.
(17) van der Laan, G.; Kirkman, I. W. *J. Phys.: Condens. Matter* **1992**, *4*, 4189.
(18) Weakliem, H. A. *J. Chem. Phys.* **1962**, *36*, 2117.
(19) Schulz, H.-J.; Thiede, M. *Phys. Rev. B* **1987**, *35*, 18.
(20) Koidl, P. *Phys. Rev. B* **1977**, *15*, 2493.
(21) Schwartz, D. A.; et al. *J. Am. Chem. Soc.* **2003**, *125*, 13205.
(22) Risbus, A. S.; et al. *Phys. Rev. B* **2003**, *68*, 205202.
(23) Marcus, M. A.; et al. *J. Synchrotron. Rad.* **2004**, *11*, 239.
(24) Newville, M. *J. Synchrotron Rad.* **2001**, *8*, 96.
(25) Kaspar, T. C.; et al. *Phys. Rev. Lett.* **2005**, *95*, 217203.
(26) Khare, N.; et al. *Adv. Mater.* **2006**, *18*, 1449.
(27) Tuan, A.; C. et al. *Phys. Rev. B* **2004**, *70*, 054424.
(28) Berciu, M.; Bhatt, R. N. *Phys. Rev. Lett.* **2001**, *87*, 107203.
(29) Coey, J. M. D.; Venkatesan, M.; Fitzgerald, C. B. *Nat. Mater.* **2005**, *4*, 173.
(30) Lee, E.-C.; Chang, K. J. *Phys. Rev. B* **2004**, *69*, 085205.

NL0626939